MEDWIN PUBLISHERS
Committed to Create Value for Researchers

The Comprehensive Morphological Criteria for the Diagnosis of Subclinical Bacterial Maternal-Fetal Infection in Offspring

Talapova PS*, Sorokina IV, Markovskii VD, Tovazhnianska VD, Sakal AO and Zvierieva IS

Department of Pathological Anatomy, Kharkiv National Medical University, Kharkiv, Ukraine

*Corresponding author: Polina Talapova, MD, PhD student, Department of Pathological Anatomy, Kharkiv National Medical University, Ukraine, Email: polina.talapova@gmail.com

Abstract

The paper presents study materials devoted to determining the morphofunctional state of progeny's organs developed under subclinical bacterial maternal-fetal infection (MFI) in order to define the comprehensive diagnostic criteria of this pathology. The rat models of subclinical MFI caused separately by *E. coli*, *S. aureus*, and *K. pneumoniae* were used, the set of diagnostic tools (histopathological staining of paraffin sections of aorta (AO), pulmonary artery (PA), thyroid (TG), and adrenal glands (AG), liver (LV) of fetuses with H&E, Mallory's trichrome and Van Gieson's methods, optical microscopy, morphometry, and immunofluorescence with the use of ImageJ software) was applied. Statistical analysis was performed in Microsoft Excel 365 and R. Depending on the organ, the null hypothesis was rejected when $p<0.05$ or $p<0.001$. The assemblage of statistically significant diagnostic parameters of the subclinical MFI damaging effect in offspring's organism was determined: for AO and PA – endotheliocyte's height, the optical density of fluorescence (ODF) of CD34-positive cells, type III and IV collagens; for TG – thyrocyte's height, nuclear-cytoplasmic ratio (NCR), follicle's square, T4 OD; for AG – adrenocorticocytes' density in zona glomerulosa, adrenocorticocyte's NCR, cortisol ODF in zona fasciculata; for LV - hepatocytes' density, NCR, the absolute number of IL-6 producing cells. Conclusion: in this study, we have proved the presence of pathomorphological substrate and defined dynamics of morphofunctional changes forming in the fetal organism under the bacterial MFI that enables the use of obtained values as diagnostic criteria of this pathology.

Keywords: Infectious Disease Transmission; Vertical; Pregnancy Complications; Infectious; Morphological and Microscopic Findings; Fetus; *Escherichia coli*; *Staphylococcus aureus*; *Klebsiella pneumoniae*

Introduction

Nowadays, intrauterine infection (IUI) accounts for 11 to 45% of perinatal mortality [1] and has a variety of complications which are represented by intrauterine growth retardation, miscarriage, premature labor, acute and persistent infections in newborns along with a late diagnosis of severe illnesses leading to different disabilities [2,3]. Thus IUI and related conditions have a strong negative social-economic impact on society.

On the one hand, the high incidence rate of IUI can be explained by the deteriorating health of the population and antimicrobial resistance of bacterial infectious agents [4,5]. On the other hand, the increase in perinatal infectious pathology can be associated with the improvement of diagnostic methods and more accurate processing of health care data.

The Comprehensive Morphological Criteria for the Diagnosis of Subclinical Bacterial Maternal-Fetal Infection in Offspring

J Human Anat

Intrauterine infections can be diagnosed in several ways: via positive blood or amniotic fluid culture, positive polymerase chain reaction, and histologically confirmed chorioamnionitis [6]. However, a lot of bacterial infections of mothers are subclinical or even asymptomatic; thereby in such cases to diagnose the development of the maternal-fetal infection accompanied by a sudden unexpected death in infancy using such methods is not always possible.

Interestingly, that according to the standard protocol for obstetric care of «Perinatal Infections» approved by the Order of the Ministry of Health of Ukraine [7], the terms «intrauterine infectioning» and «intrauterine infection» are not synonymous, inasmuch as the first reflects the fact of invasion of a microorganism into the fetus, which does not lead to the development of pathological changes or clinical manifestation. Thus, to diagnose intrauterine infection in pathological anatomy, a morphological substrate of the infectious damaging effect has to be obligatorily present.

In addition, in the available literature, there are still no complex pathomorphological benchmarks to confirm the onset of the subclinical bacterial MFI in an offspring's organism during postmortem examination. Therefore, the need for this study is justified by the urgency of the problem and the lack of the respective knowledge.

Aim of Study

This study was designed in order to experimentally reproduce the subclinical bacterial maternal-fetal infection, determine the morphofunctional states of offspring's organs developed under and to define the comprehensive diagnostic criteria of this pathology.

Materials and Methods

At the laboratory of the Department of Pathological Anatomy and the Experimental Biological Clinic of Kharkiv National Medical University, we conducted an experimental study on female rats of the Wistar Albino Glaxo (WAG) population with a subsequent pathomorphological examination of offspring's organs, which are crucial for the young organism's development, but which have not yet been studied from this perspective, namely the aorta (AO), pulmonary artery (PA), thyroid gland (TG), adrenal glands (AG), and liver (LV). Four experimental groups were randomly selected, in which female rats (n=95) were or were not exposed to the *E. coli, S. aureus*, or *K. pneumoniae* infections before pregnancy. Groups of histological samples from fetuses (n=43) obtained at the end of the experiment were randomly assigned according to the age and the experimental influence during the intrauterine development. The summary of the grouping in the study is presented in Table 1.

Animal Type	#	Group Name	Exposure Type	Number Of Animals Per Group	Number of Extracted Organ Blocs
Female rat (mother)	1.1	MEC	*E. coli* infection	25	n/a
	1.2	MKP	*K. pneumoniae* infection	25	n/a
	1.3	MC	Placebo	10	n/a
	1.4	MSA	*S. aureus* infection	25	n/a
Male rat (father)	2.1	FTHC	n/a	4	n/a
	2.2	FTHEC	n/a	6	n/a
	2.3	FTHKP	n/a	6	n/a
	2.4	FTHSA	n/a	6	n/a
Fetus rat (offspring)	3.1	FEC	Subclinical MFI caused by *E. coli*	10	10
	3.2	FKP	Subclinical MFI caused by *K. pneumoniae*	9	9
	3.3	FC	Placebo in mother	10	10
	3.4	FSA	Subclinical MFI caused by *S. aureus*	8	8
Total				144	37

Table 1: Groups of experimental and pathomorphological studies in the research.
- n/a – not applicable

The study design was based on the patented method of modeling the intrauterine infection in a fetus and newborn as the consequence of a subacute infectious-inflammatory process of a mother [8].

According to the recommendations of the "Animal Research: Reporting of in Vivo Experiments" (ARRIVE) guideline [9], we set the endpoints of the experiment presented in Table 2.

Endpoint Name	Description
Secondary milestone 1	Reproduction of prolonged subacute infectious inflammatory process with subclinical course in the abdominal cavity of female WAG rats before pregnancy: Day 0 – sensitization of female rats by a single SC injection of a suspension of heat-killed cells of reference strains of E. coli (ATCC 25922 (F50)), *S. aureus* (ATCC 25923) and *K. pneumoniae* (NCTC 5055) in a dose of 0.1 ml with a density of 1U, 3U, and 1U respectively (according to the McFarland standard). 10th, 20th, and 30th days – modelling of maternal infection with subacute inflammation by intraperitoneal injection of a suspension of microbial cells diluted in 0.1 ml of 20% mannitol solution in the amount of $300 \times 10^6 – 1 \times 10^9$ for *E. coli*, $200 \times 10^6 – 800 \times 10^6$ for *S. aureus*, and $100 \times 10^6 – 500 \times 10^6$ for MKP group.
Secondary milestone 2	Fertilization: 32nd day - setting down of males (2 per 1 cage) in order to fertilize females with estrus through mating, collection of vaginal swabs to confirm the fact of fertilization.
Secondary milestone 3	Obtaining of rat offspring: 51st day (20th day of pregnancy): euthanasia of female rats via injection of 5% solution of sodium thiopental (UA/3916/01/01) with subsequent decapitation, removal, and autopsy of previously decapitated fetuses to obtain their organs.
Primary milestone 1	Confirmation of the development of MFI by histological examination of rat placentas.
Primary milestone 2	Extraction of organs from rat fetuses suffering from the subclinical MFI caused by *E. coli, S. aureus, K. pneumoniae.*
Primary milestone 3	Pathomorphological examination of obtained specimens with subsequent collection and analysis of experimental data.

Table 2: The endpoints of the experiment.

The care, experimentation, euthanasia, and disposal of biological waste were performed in accordance with the Directive 2010/63/EU of the European Parliament and of the Council of 22 September 2010 on the protection of animals used for scientific purposes and principles of Good Laboratory Practice [10]. Pathomorphological study of organ blocs of rat offspring was done with the use of a set of methods: the preparation of paraffin blocks and sections, staining with hematoxylin and eosin (as a principal stain), Mallory's trichrome (for collagens and cytoplasm visualization) and Van Gieson's methods (to differentiate collagens from other types of connective tissues and for better contouring of mesenchyma), optical microscopy via Carl Zeiss PrimoStar microscope and microphotography on a Carl Zeiss Axiocam 105 color camera with subsequent morphometry using ImageJ software (versions from 1.52a to 1.52o), which is widely used for such a purpose [11]. All images were calibrated and scaled, and then regions of interest were annotated with the use of "Magnifying glass" and "Freehands selection" tools. Measurements used to define the cell height, squares of cytoplasm, and nucleus for the determination of nuclear-cytoplasmic ratio (NCR), which is known to be an indicator of cellular activity [12]. Listed measures were made automatically after respective settings by enabled checkboxes of Area, Perimeter, and Feret's diameter and "Ctrl+M" keyboard shortcut.

Also, we performed immunofluorescence study of such well-known morphofunctional parameters as the CD34 expression by endotheliocytes, production of collagen type III (IMTEK, Ltd) and IV (Novocastra Laboratories Ltd), activity of follicular epithelium and renal cortex in the form of T4 (Chemicon International) and cortisol (Novocastra Laboratories Ltd) synthesis respectively, and hepatic macrophages' function via IL-6 (Novocastra Laboratories Ltd) production [13-17]. The estimation of optical density of fluorescence of monoclonal antibodies (MoAb) of substances listed above was carried out with the use of Carl Zeiss Axioskop 40 FL microscope, microphotography by a digital camera Canon A5 and analysis of images in the ImageJ by mathematical algorithm of maximum entropy threshold.

Obtained values of morphometric parameters were evaluated using statistical tools of Microsoft Excel 365 and R (license: GNU GPL v2, packages: dplyr, ggplot2, pastecs, graphics) – a software environment for statistical

computing and graphics [18]. We defined measures of the central tendency, dataset variability, performed the Shapiro-Wilk test for normality, Bartlett's test to check equality of variances across multiple samples, the Box-Cox method for normalization of data, one-way analysis of variance (ANOVA) to compare mean values of quantitative variables, post hoc Tukey's test to control the family-wise error, and correlation analysis to evaluate the strength *of the* relationship between two quantitative variables. The null hypothesis was rejected if the probability of error did not exceed the Type I error which was set as 0.05 and 0.001 ($p < 0.05$ and $p < 0.001$) depending on the choice of the researcher, investigated a particular organ.

This paper is a final summary of the research work of the Department of Pathological Anatomy of Kharkiv National Medical University «Pathological anatomy of the fetus and newborn with maternal-fetal infection» (UDC: 616 - 091 - 053.12 / .31: 618.3 - 06 - 022.7: 001.89) based on separate scientific efforts which are thematically connected.

Results

The interim results of the study, reflecting all morphofunctional parameters of AO, PA, TG, AG, and LV in offspring's organism under the impact of the subclinical MFI caused either *E. coli or S. aureus or K. pneumoniae* infections, have been published earlier in scientific periodic. The final results of statistical significance ($p < 0.05$ for AO, PA, LV; $p < 0.001$ for TG and AG), which were different from those obtained in physiological fetal growth, are presented in this paper. We considered them the most important criteria for the pathomorphological diagnosis of the subclinical bacterial MFI in offspring's organism with the determination of threshold *pathological value* (TPV) and *pathological trend* (PT) displayed in Table 3. TPV characterizes a quantitative borderline value of a morphofunctional parameter which defines the starting point to the PT application. In turn, PT value can be either "↓" which stands for "and less" describing the decrease of the parameter or "↑" which stands for "and higher" describing the increase of it.

Organ	#	MFS criterion short name	Criterion full name	TPV	PT	Unit of measure	p-value
Aorta (AO)	1	H_end	Height of the endotheliocyte	3.16±0.07	↓	µm	p<0.05
	2	ODF_CD34	ODF of CD34-positive cells	0.6±0.06	↑	U	p<0.05
	3	OD_cllg3	ODF of the type III collagen	0.76±0.08	↑	U	p<0.05
	4	OD_cllg4	ODF of the type IV collagen	0.76±0.15	↑	U	p<0.05
Pulmonary artery (PA)	5	H_end	Height of the endotheliocyte	6.66±0.51	↓	µm	p<0.05
	6	ODF_CD34	ODF of CD34-positive cells	0.62±0.44	↑	U	p<0.05
	7	OD_cllg3	ODF of the type III collagen	0.66±0.46	↑	U	p<0.05
	8	OD_cllg4	ODF of the type IV collagen	0.84±0.18	↑	U	p<0.05
Thyroid gland (TG)	9	H_thyr	Height of the thyrocyte	10.353 ±0.077	↑	µm	p<0.001
	11	NCR_thyr	NCR of the thyrocyte	0.651 ±0.091	↓	µm	p<0.001
	10	S_fol	Square of follicle	445.012 ±2.313	↑	µm^2	p<0.001
	12	ODF_T4	ODF of thyroxine	80.652 ±0.217	↑	U	p<0.001
Adrenal glands (AG)	13	Glom_DNS_cell	Cell density in the zona glomerulosa	25.31±0.23	↓	Copies per visual field	p<0.001
	14	Glom_NCR	NCR of the adrenocorticocyte	0.389 ±0.009	↑	n/a	p<0.001
	15	ODF_CTS_Fasc	ODF of cortisol in the zona fasciculata	0.93 ±0.01	↑	U	p<0.001
Liver (LV)	16	NCR_hep	NCR of the hepatocyte	0.26 ±0.01	↓	n/a	p<0.05
	17	S_hep	Square of the hepatocyte	123.27 ±2.9	↓	µm^2	p<0.05
	18	IL6_cell	Absolute number of IL-6 producing cells	1.96±0.21	↑	copies	p<0.05

Table 3: The list of the key morphofunctional diagnostic criteria of the offspring's organism developed under the subclinical bacterial MFI.

Talapova PS, et al. The Comprehensive Morphological Criteria for the Diagnosis of Subclinical Bacterial Maternal-Fetal Infection in Offspring. J Human Anat 2021, 5(1): 000156.

Copyright© Talapova PS, et al.

Several trends listed above, which demonstrated the morphofunctional behavior of organs obtained from rat offspring developed under the subclinical bacterial MFI, are shown in the form of histopathology slides in Figure 1.

Discussion

In AO and PA, there were analogical PTs in the form of the decrease in H_end that, according to the literature sources, can be a benchmark of the predisposition to endotheliopathy [19]. In parallel, the increase in CD34 expression was registered, that is directly in line with previous studies stated that such pattern indicates enhanced angiogenesis which carried out by the endothelial colony-forming cells, accelerating normal development [20]. Furthermore, there was the increase in ODF of type III and IV collagens which is considered to be a marker of the intensified maturation of any vascular structure during fetal growth [21]. But it must

be pointed out that some authors believe that accelerated collagenogenesis might be connected to peculiarities of the physiology of rats [22].

In TG, there was the increase of ODF_T4, H_thyr, and S_fol that ties well with previous studies wherein such changes indicated enhanced functional activity of the gland [23]. However, there was a decrease in NCR, which, according to the literature, can be a criterion of the accelerated maturation of the gland [24]. In combination, such findings go beyond previous reports.

In AG, there was the increase in ODF_CTS along with NCR in the zona glomerulosa. Some researches stated that such a pattern demonstrates the increase in the functional activity [25]. But, in parallel, our results showed the adrenal cortex hypoplasia which was reflecting by the decrease in DNS_cell.
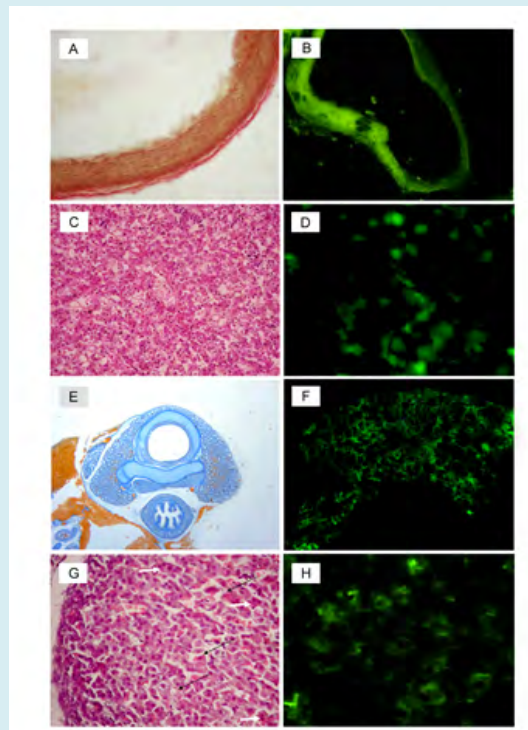

Figure 1: Histopathology images obtained from rat progeny developed under the subclinical bacterial MFI: **A** – Increased acidophilia of PA's adventitial membrane of a rat offspring suffering from the subclinical MFI caused by *E. coli* – index of increased collagenogenesis, Van Gieson's stain, ×400; **B** – The unevenly thickened wall of PA with intensive fluorescence of type III collagen. MoAb to Col3 *K. pneumoniae* infection, ×1000; **C** – LV of a rat fetus infected with E. coli: plethora of the central vein, deformation of hepatic laminae, dystrophic and necrotic changes in hepatocytes. H&E stain, ×200; **D** – LV of a rat fetus infected by E. coli: fluorescence of IL-6-producing cells, MoAb to IL-6, ×1000; **E** – TG of a rat fetus suffering from the subclinical MFI caused by *S. aureus*: acceleration of follicular parenchyma development, characteristic sponge-like appearance, Mallory's trichrome stain, ×40; **F** – Intensive fluorescence of T4 in the developing parenchyma of TG of a rat fetus with MFI caused by S. aureus, MoAb to T4, 100; **G** – Giant cells (white arrows), foci of cytolysis and resorption (black arrows) in the fascicular and fetal zones of the cortex of the AG of a fetus rat infected by *S. aureus*, H&E, ×400; **H** – The fluorescence of cortisol is affected in the fascicular zone of the rat fetus suffering from the subclinical MFI caused by S. aureus. MoAb to cortisol, ×650.

In LV, there were similar morphological findings represented by increased S_hep and NCR_hep, which can be evidence of both – intensified maturation, on the one hand, and decreased synthetic function, on the other hand [26,27]. Additionally, we revealed the initiation of cell injury in the form of increased IL6_cell [28].

Therefore, the assemblage of statistically significant pathomorphological diagnostic criteria of the subclinical bacterial MFI in offspring's organism was determined: for AO and PA - height and width of endotheliocyte together with the optical density of fluorescence (ODF) of CD34-positive cells, type III collagen and type IV collagen; for TG - the height and nuclear-cytoplasmic ratio (NCR) of the thyrocyte, square of the follicle, ODF of T4, TNF, IL-6; for AG - cell density in the zona glomerulosa, NCR of the adrenocorticocyte, ODF of cortisol in the zona fasciculata; for LV - NCR of the hepatocyte, hepatocytes' density, and the absolute number of IL-6 producing cells.

Conclusions

In this study, we have performed a comparative analysis of offspring's morphofunctional parameters between bacterial maternal-fetal infections with subclinical course caused separately by E. coli, K. pneumoniae, and S. aureus, and physiological ontogenesis. Furthermore, we have proved the presence of pathomorphological substrate and defined dynamics of morphofunctional changes forming in the fetal organism under the bacterial MFI. This statistically validated empirical evidence enables the use of obtained values as diagnostic criteria of mentioned pathology.

Conflict of Interests

The authors have no conflict of interest to declare.

References

1. Shherbyna MO, Vygivs'ka LA, Kapustnyk NV (2016) Intrauterine infection as a reason of pathological conditions of the perinatal period. Perinatology and pediatrics 2(66): 65-69.

2. Boushra M, Farci F (2020) Antepartum Infections. In StatPearls. StatPearls Publishing.

3. Bauer ME, Bateman BT, Bauer ST, Shanks AM, Mhyre JM (2013) Maternal sepsis mortality and morbidity during hospitalization for delivery: temporal trends and independent associations for severe sepsis. Anesthesia and analgesia 117(4): 944-950.

4. Bhutta ZA, Guerrant RL, Nelson CA (2017) Neurodevelopment, Nutrition, and Inflammation: The Evolving Global Child Health Landscape. Pediatrics 139(Suppl 1): S12–S22.

5. Dadgostar P (2019) Antimicrobial Resistance: Implications and Costs. Infection and drug resistance 12: 3903-3910.

6. Goldenberg RL, Culhane JF, Johnson DC (2005) Maternal infection and adverse fetal and neonatal outcomes. Clinics in perinatology 32(3): 523-559.

7. Ministry of health of Ukraine (2006) on approval of the clinical protocol for obstetric care "Perinatal infections".

8. Markovskii VD, Sorokina IV, Myroshnichenko MS, Pliten OM, Mishina MM, et al. (2015) Method of modeling intrauterine infection of the fetus and newborn as a consequence of subacute infectious-inflammatory process of the mother. Ukraine patent 108806 G09B 23/28 (2006.01).

9. Kilkenny C, Browne WJ, Cuthill IC, Emerson M, Altman DG (2010) Improving bioscience research reporting: the ARRIVE guidelines for reporting animal research. PLoS biology 8(6): e1000412.

10. Ito K, Someya H (2019) Good Laboratory Practice: Initial Development, Necessity, and Issues of Data Reliability in Basic Research. Journal of the Pharmaceutical Society of Japan 139(6): 875-879.

11. Handala L, Fiore T, Rouillé Y, Helle F (2019) QuantIF: An ImageJ Macro to Automatically Determine the Percentage of Infected Cells after Immunofluorescence Viruses 11(2): 165.

12. Mukherjee RN, Sallé J, Dmitrieff S, Nelson KM, Oakey J, et al. (2020) The Perinuclear ER Scales Nuclear Size Independently of Cell Size in Early Embryos. Developmental cell 54(3): 395-409.

13. Prasad M, Corban MT, Henry TD, Dietz AB, Lerman LO, et al. (2020) Promise of autologous CD34+ stem/progenitor cell therapy for treatment of cardiovascular disease. Cardiovascular research 116(8): 1424-1433.

14. Hušáková M, Bay-Jensen AC, Forejtová Š, Zegzulková K, Tomčík M, et al. (2019) Metabolites of type I, II, III, and IV collagen may serve as markers of disease activity in axial spondyloarthritis. Scientific reports 9(1): 11218.

15. Ribeiro L, Silva JF, Ocarino NM, Souza CA, Melo EG, et al. (2018) Excess Maternal Thyroxine Alters the Proliferative Activity and Angiogenic Profile of Growth Cartilage of Rats at Birth and Weaning. Cartilage 9(1): 89-103.

16. Shalaby AM, Aboregela AM, Alabiad MA, El Shaer DF (2020) Tramadol Promotes Oxidative Stress, Fibrosis, Apoptosis, Ultrastructural and Biochemical alterations in the Adrenal Cortex of Adult Male Rat with Possible Reversibility after Withdrawal. Microscopy and microanalysis: Microsc Microanal 26(3): 509-523.

17. Schmidt-Arras D, Rose-John S (2016) IL-6 pathway in the liver: From physiopathology to therapy. Journal of hepatology 64(6): 1403–1415.

18. Li Y, Guo M, Li C, Chen C, Lu F (2019) Meta-analysis of acute health effects caused by atmospheric particulate matter and the implementation with R software. Journal of hygiene research 48(2): 312-319.

19. Borzenko I, Konkov D, Kondratova I, Basilayshvili O, Gargin V (2019) Influence of endotheliopathy of spiral arteries on placental ischemia. Georgian medical news 296: 131-134.

20. Tasev D, Konijnenberg LS, Amado-Azevedo J, van Wijhe MH, Koolwijk P, et al. (2016) CD34 expression modulates tube-forming capacity and barrier properties of peripheral blood-derived endothelial colony-forming cells (ECFCs). Angiogenesis 19(3): 325-338.

21. Sorokina IV, Myroshnychenko MS, Kapustnyk NV, Khramova TO, Dehtiarova OV, et al. (2018) Morphological characteristics of kidneys connective tissue of mature fetuses and newborns from mothers, whose pregnancy was complicated by preeclampsia of varying degrees of severity. Wiad lek 71(3 pt 1): 579-587.

22. Kaluzhyna OV (2015) The influence of chronic intrauterine hypoxia on the morphological state of the pulmonary artery in fetuses and newborns (experimental study). Bulletin of the Ukrainian Medical Dental Academy 15(1/49): 168-171.

23. Ali Rajab NM, Ukropina M, Cakic-Milosevic M (2017) Histological and ultrastructural alterations of rat thyroid gland after short-term treatment with high doses of thyroid hormones. Saudi journal of biological sciences 24(6): 1117-1125.

24. Vaickus LJ, Tambouret RH (2015) Young investigator challenge: The accuracy of the nuclear-to-cytoplasmic ratio estimation among trained morphologists. Cancer cytopathology 123(9): 524-530.

25. Thau L, Gandhi J, Sharma S (2020) Physiology, Cortisol. In: StatPearls. StatPearls Publishing.

26. Fomenko EV, Yvanov AV, Bobyntsev YY, Belyh AE, Garbelotto NK, et al. (2017) Selank effect on the morphological state of rat hepatocytes under acute immobilization stress. Kursk Scientific and Practical Bulletin "Man and His Health" 4: 108-114.

27. Kulynych GB (2019) Morphometrical changes of the hepatocytes under influence of the pesticide 2,4-d and after intragastric correction by glutargin. Precarpathian bulletin of the shevchenko scientific society pulse 4(24): 147-154.

28. Han R, Zhang F, Wan C, Liu L, Zhong Q, et al. (2018) Effect of perfluorooctane sulphonate-induced Kupffer cell activation on hepatocyte proliferation through the NF-κB/TNF-α/IL-6-dependent pathway. Chemosphere 200: 283-294.